La(Ni,Fe)O$_3$ Stability in the Presence of Cr Species - Solid State Reactivity Study

M. Stodolny[a], F.P.F. van Berkel[a], B.A. Boukamp[b]

[a]Energy Research Centre of the Netherlands (ECN), SOFC R&D
Westerduinweg 3, 1755 ZG Petten, The Netherlands
[b]Inorganic Materials Science, Faculty of Science and Technology, University of Twente
P.O. Box 217, Enschede 7500 AE, The Netherlands

The solid-state reactivity between La(Ni$_{0.6}$Fe$_{0.4}$)O$_3$ (LNF) and Cr$_2$O$_3$ in the IT-SOFC operating temperature range of 600-800ºC has been investigated using XRD analysis. Because LNF material can be used as a cathode, as a current collecting layer and/or an interconnect coating, a thorough investigation of its chemical stability is of importance for SOFC systems utilizing ferritic stainless steel interconnects. This study demonstrates the intrinsic instability of LNF when exposed to direct contact with Cr$_2$O$_3$ at 800ºC. It has been observed that Cr enters the perovskite phase, replacing first Ni and then Fe already after 200 h. The rate of the Cr reaction with LNF depends on temperature and exposure time. After 1000 h at 600ºC no reaction products could be detected with XRD. Although this is a promising result, long-term testing under fuel cell operating conditions is needed to prove LNF as a viable IT-SOFC cathode material.

Introduction

For intermediate temperature solid oxide fuel cells (IT-SOFCs), chromia-forming ferritic stainless steels can be used as bipolar plates, enhancing ease of fabrication, workability and cost-effectiveness of the SOFC interconnects. However, the evaporation of Cr-oxide and oxyhydroxide species from these metal separator plates in an oxygen-rich atmosphere is known to be highly detrimental to the functioning of the state-of-the-art SOFC cathodes. This may be due to poisoning of electrochemically active sites or the formation of secondary phases with low electrical conductivity. Especially cathode materials containing Sr, Mn and/or Co, such as (La,Sr)MnO$_3$ (LSM) or (La,Sr)CoO$_3$ (LSC) perovskites, are poisoned by volatile Cr-species (1,2).

It has recently been found that La(Ni,Fe)O$_3$-based cathodes have higher resistance against chromium poisoning (3,4). Of particular interest is the component La(Ni$_{0.6}$Fe$_{0.4}$)O$_3$ (LNF) which exhibits high electronic conductivity and a thermal expansion coefficient matching that of the zirconia electrolyte (5). Optimization of the microstructure of the LNF-cathode has been shown to result in enhanced electrochemical performance (6). However, recent endurance test data, obtained at ECN on SOFC with LNF cathode at operating temperatures of 800-850ºC, showed degradation in cell performance when tested in combination with a metallic interconnect as a chromium source (7), despite the Cr-resistance claimed in the literature.

Besides its application as cathode material, LNF can be used as a current collecting layer and/or an interconnect coating. As such, a thorough understanding of the true extent of LNF chemical stability in the presence of Cr species is vital for its application in SOFC systems when ferritic steel interconnects are used. The transport of Cr-species is known to take place along two pathways, i.e. through vapor phase transport or through direct solid state diffusion (2). The present study deals with the solid-state reactivity between LNF and Cr_2O_3 in the IT-SOFC operating temperature range of 600-800ºC. To this end, mixtures of LNF and Cr_2O_3 were heated at 600-800ºC and possible changes in the phase composition were analyzed by means of X-ray diffraction.

Experimental

Powders of $La(Ni_{0.6}Fe_{0.4})O_3$ (Praxair, 99.9%) and Cr_2O_3 (Alfa Aesar, 99%) were used for the determination of the reactivity of Cr_2O_3 with $La(Ni_{0.6}Fe_{0.4})O_3$. The available 'as received' $La(Ni_{0.6}Fe_{0.4})O_3$ powder contained trace amounts of non-reacted La_2O_3, which disappeared after heat treatment at 800ºC for 1 h. Therefore, in all experiments this pretreated powder was used. The abbreviation LNF refers to this pretreated powder. Both LNF and Cr_2O_3 powders were thoroughly mixed in weight ratios of 10:1, 10:3 and 10:5. The mixing procedure included overnight rolling of PET bottles containing the powder mixture and zirconia milling balls. Subsequently, these powder mixtures were heated in ambient air at 800ºC for 200 h and at 600ºC for 200 or 1000 h. The heating and cooling rate was 100ºC/h. The resulting samples were examined at room temperature by powder X-ray diffraction (XRD) using a Philips X'Pert diffractometer, equipped with the X'Celerator, operating with CuKα radiation in steps of 0.02º (2θ) and 10 s counting time in the 2θ range between 10º and 140º. The lattice parameters were obtained by fitting the XRD spectra using the so-called "Le Bail" method (8) implemented in the LHPM-Rietica software (9).

As a reference, the thermal stability of a pure LNF sample was investigated by means of prolonged heating (at 800ºC) followed by XRD-analysis and by in-situ high temperature-XRD (HT-XRD) using a Bruker D8 Advance diffractometer equipped with MRI chamber as heating device and operating in Bragg Brentano mode.

To check whether full thermodynamic equilibrium had been reached in the LNF-Cr_2O_3 powder mixtures, additional heat treatments were conducted on the samples in air at 1400 ºC for 24 h. For the same reason, some perovskite compositions in the $LaNiO_3$-$LaFeO_3$-$LaCrO_3$ system were prepared via a standard solid-state reaction method and sintered in air at 1400ºC for 24 h.

Results and Discussion

This section describes the results concerning the stability of LNF in direct solid state contact with Cr_2O_3-powder at 800 and 600ºC. The thermal stability of pure LNF in this temperature regime is discussed first, followed by the XRD analysis of the reactivity between LNF and Cr_2O_3 at 800 and 600ºC, respectively.

Thermal Stability of Pure LNF

Figure 1 and Table I show the XRD patterns and cell parameters of the starting LNF material and LNF material after heating at 800ºC in air for 200 h. Prolonged heating resulted in enhanced crystallinity as compared with the starting LNF material (Fig. 1). Double splitting of the main reflection, characterizing the rhombohedral distortion of the ideal perovskite structure, was clearly visible at $32° < 2\theta < 33°$ for the LNF sample heated at 800ºC for 200 h. The resulting fitted cell parameters of both LNF samples were identical within the given errors (Table I), demonstrating that LNF remains the same phase after prolonged heating. High temperature XRD analysis in the 800-1200 ºC range shows that $La(Ni_{0.6}Fe_{0.4})O_3$ also remained in the *R-3c* rhombohedral structure, indicating the stability of the LNF phase in the given temperature regime. In all cases, neither impurities (such as NiO) nor other phases were found, which further proves the thermal stability of the LNF compound.
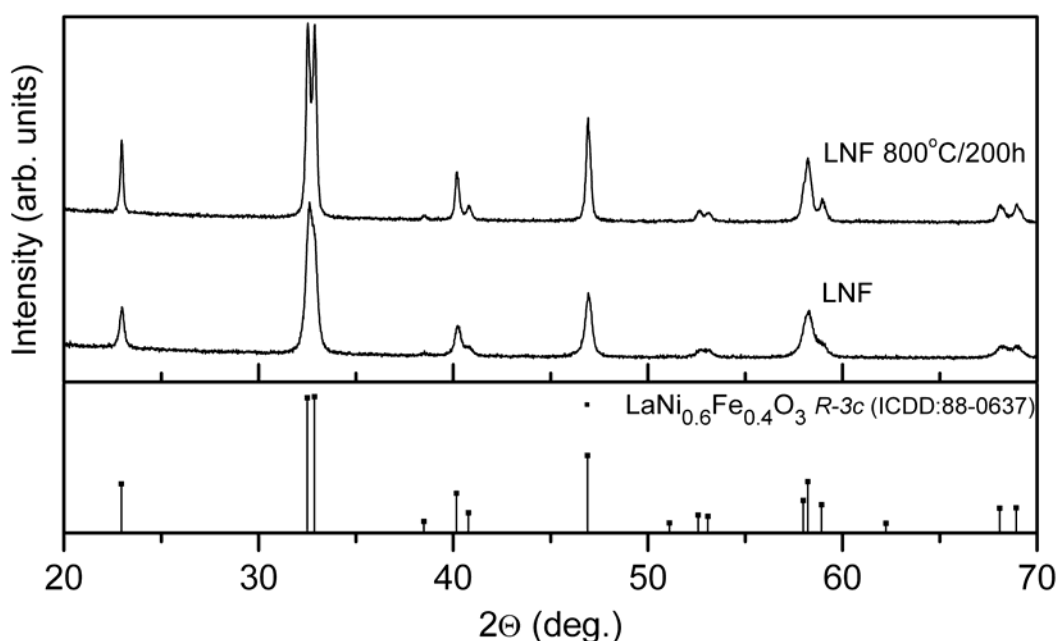

Figure 1. X-ray powder diffraction patterns of $La(Ni_{0.6}Fe_{0.4})O_3$ compound (initial LNF and LNF heated at 800ºC for 200 h).

LNF and Cr_2O_3 Reactivity at 800ºC

Mixture $10LNF +1Cr_2O_3$. For the heated mixture of $10LNF+1Cr_2O_3$, the analysis of the XRD spectra revealed cubic NiO and two perovskite phases: orthorhombic *Pbnm* and rhombohedral *R-3c* (Fig. 2). No presence of Cr_2O_3 was observed, suggesting that it had completely reacted with LNF. The fitted cell parameters of the two perovskite phases are summarized in Table I. This table shows that the rhombohedral phase has comparable cell parameters with LNF, suggesting that LNF was partly present in the mixture. As a consequence, the orthorhombic perovskite phase should contain chromium, indicating that it is highly likely to belong to the $La(Ni,Fe,Cr)O_3$ perovskite system. Actually, the presence of NiO, LNF and a $La(Ni,Fe,Cr)O_3$ perovskite phase as well as the absence of Cr_2O_3 implies that Ni was partially precipitated from the LNF perovskite lattice, whereas Cr was incorporated. The introduction of Cr into the perovskite phase seems to result in the orthorhombic perovskite phase.
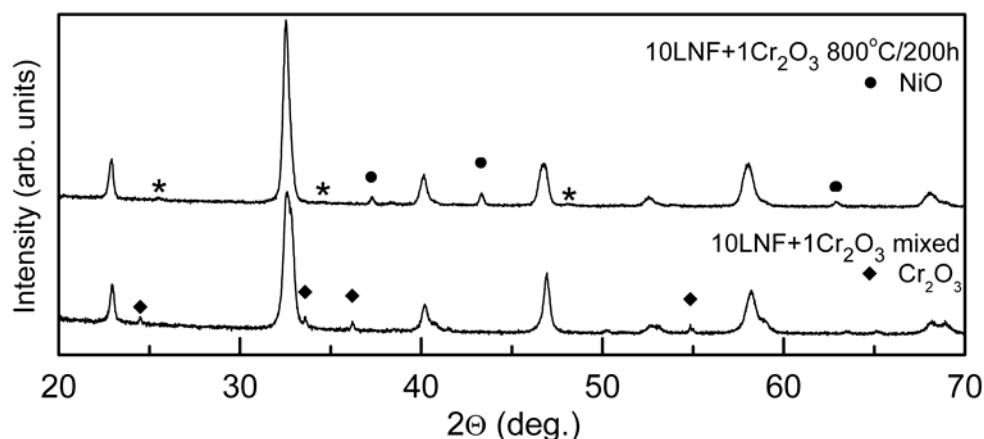
Figure 2. X-ray powder diffraction patterns of the mixture $10LNF+1Cr_2O_3$ ('only mixed' and heated at 800ºC for 200 h). Presence of the orthorhombic *Pbnm* phase is marked by * at the distinctive reflection angles where the specific Bragg reflections for the orthorhombic phase are visible.

TABLE I. Structural properties of investigated perovskites

Composition	Space group	a [Å]	b [Å]	c [Å]	V [Å]^3
LNF	*R-3c*	5,5032(9)	–	13,267(2)	347,98(9)
LNF 800 ºC/200 h	*R-3c*	5,5039(5)	–	13,267(1)	348,07(5)
$10LNF+1Cr_2O_3$ 800 ºC/200 h	*R-3c*	5,5015(4)	–	13,274(9)	347,94(4)
	Pbnm	5,5273(4)	5,4773(4)	7,8145(5)	236,58(3)
$10LNF+1Cr_2O_3$ 1400 ºC/24 h	*Pbnm*	5,5325(1)	5,5101(1)	7,7982(2)	237,72(1)
$La(Ni_{0.28}Fe_{0.40}Cr_{0.32})O_3$	*Pbnm*	5,5311(1)	5,5081(1)	7,7958(2)	237,51(1)
$La(Ni_{0.1}Fe_{0.4}Cr_{0.5})O_3$	*Pbnm*	5,5352(1)	5,55163(1)	7,8026(2)	238,24(1)
$La(Ni_{0.5}Fe_{0.4}Cr_{0.1})O_3$	*Pbnm*	5,5326(1)	5,4735(1)	7,7574(2)	234,44(1)
$10LNF+3Cr_2O_3$ 800 ºC/200 h	*Pbnm*	5,5132(4)	5,4897(6)	7,8070(4)	236,29(3)
$10LNF+5Cr_2O_3$ 800 ºC/200 h	*Pbnm*	5,5066(5)	5,4885(5)	7,8093(7)	236,02(4)

Le Bail full pattern decomposition method yielded in all cases the reliability factors of R_p = 3÷4% and R_{wp} = 5÷6% with accuracy of the fit χ^2 = 1.3÷1.4.

The observed reactivity of LNF with Cr_2O_3 is in agreement with thermodynamic calculations (10), which predict the instability of LNF in combination with Cr_2O_3 and the precipitation of NiO. However, a similar study (11) suggests that only the rhombohedral LNF and $NiCr_2O_4$ were formed. The difference in results with (11) is hard to explain, but the fact that a relatively large NiO-impurity was reported in their initial LNF might result in different reactivity behavior.

To investigate whether the $10LNF+1Cr_2O_3$-mixture had reached thermodynamic equilibrium at 800ºC, the same mixture was heated in air at an elevated temperature of 1400 ºC for 24 h in order to accelerate the reaction between the two components. Figure 3 shows X-ray diffraction peaks evolution in the 2θ range of 39-41º of LNF and the mixture of $10LNF+1Cr_2O_3$ heated at different temperatures. The chosen 2θ range of 39-41º is characteristic for the detection of the presence of rhombohedral and orthorhombic perovskite phases (12). For the pure LNF, heated at 800ºC for 200 h, two single peaks appearing in the studied 2θ range can be indexed as 202 and 006 of the rhombohedral phase. In the sample $10LNF+1Cr_2O_3$ heated at 800ºC for 200 h, the small

006 peak was very weak and the single peak 202 began evolving into doublet peaks, indicating the presence of both rhombohedral and orthorhombic perovskite phases. For the same mixture of 10LNF+1Cr$_2$O$_3$ but heated at 1400ºC for 24 h, the single peak changed completely into the doublet peaks indexed as 022 and 202 of the orthorhombic phase. No peak identified as rhombohedral phase was detected. It appears that the formation of the orthorhombic phase is the thermodynamically stable situation. As a consequence, this indicates that the sample 10LNF+1Cr$_2$O$_3$ heated at 800ºC for 200 h has not yet reached equilibrium. For the sample sintered at 1400ºC for 24 h, the composition of the orthorhombic perovskite phase can be calculated by completely replacing Ni in the LNF lattice by chromium, resulting in the composition La(Ni$_{0.28}$Fe$_{0.40}$Cr$_{0.32}$)O$_3$. As a final check, this perovskite phase was prepared by means of a standard solid-state reaction method with a final sintering step in air at 1400 ºC for 24 h. The resulting X-ray pattern (see Figure 3 and Table I) indicates that the composition La(Ni$_{0.28}$Fe$_{0.40}$Cr$_{0.32}$)O$_3$ exists as a single phase with an orthorhombic *Pbnm* structure.
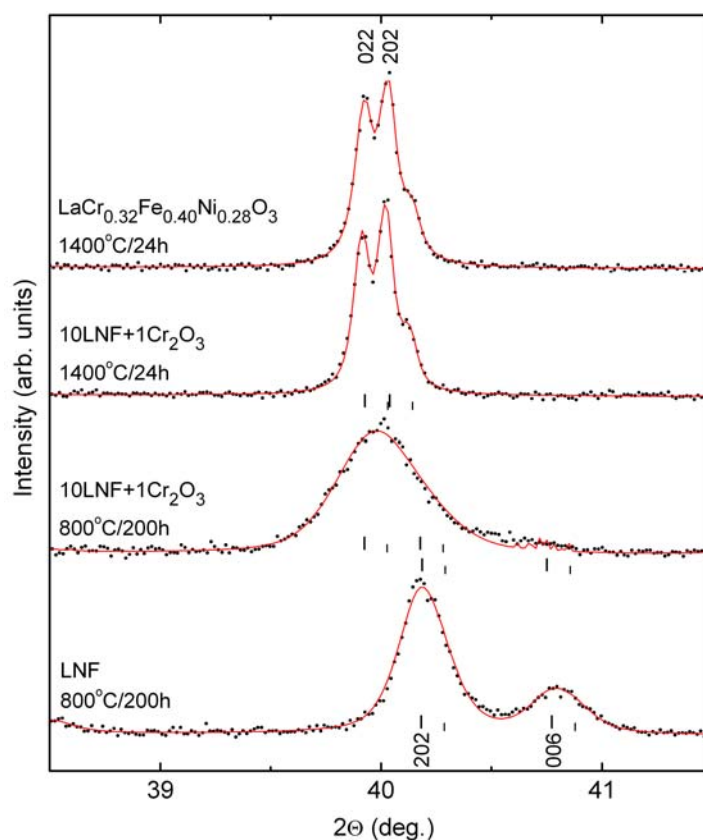

Figure 3. X-ray diffraction peaks variation in the 2θ range 39-41º of LNF and the mixture 10LNF+1Cr$_2$O$_3$ heated at different temperatures. The continuous line is the Le Bail fit using the space group *R-3c* and/or *Pbnm*. For the doublet peaks 022 and 202, additional splitting due to Kα$_1$ and Kα$_2$ radiations is visible. The longer and shorter bars correspond to Kα$_1$ and Kα$_2$ radiation, respectively.

So far, no mention has been made in the literature of investigations concerning the perovskites belonging to the La(Ni,Fe,Cr)O$_3$ system. Therefore, three different compositions of the LaFe$_{0.4}$(Ni$_{0.6-x}$Cr$_x$)O$_3$ series were prepared to further confirm the existence of a perovskite solid solution phase when Ni is replaced by Cr in LNF. X-ray diffraction analysis shows that the LaFe$_{0.4}$(Ni$_{0.6-x}$Cr$_x$)O$_3$ series samples with x= 0.1, 0.32, 0.5 adopted orthorhombic structure with the space group *Pbnm*. An increase in cell

parameters and cell volume following Vegard's law was observed on the successive replacement of the smaller nickel-ion by the larger chromium-ion. The standard six-coordinate ionic radius of Ni^{3+} and Cr^{3+} is 0.60 Å and 0.645 Å, respectively (13).

Figure 4 shows the increase in normalized volume (V_{cell}/Z, where Z is the number of formulas per unit cell) with increasing Cr-content. This figure also provides the normalized volume data of the orthorhombic and rhombohedral perovskite phase of the $10LNF+1Cr_2O_3$ sample heated at 800ºC for 200 h. It can be observed that the normalized volume of the rhombohedral phase in the mixture is equal to the normalized volume of LNF. The orthorhombic phase in the mixture has slightly lower normalized volume than the expected orthorhombic perovskite $La(Ni_{0.28}Fe_{0.40}Cr_{0.32})O_3$, indicating a lower Cr-content - which is in agreement with the fact that this mixture still contains the rhombohedral LNF and has not yet reached equilibrium.

Figure 4 also shows that an increase in the sintering temperature to 1400ºC/24 h for the $10LNF+1Cr_2O_3$ mixture results in a perovskite cell volume corresponding with $La(Ni_{0.28}Fe_{0.40}Cr_{0.32})O_3$, which proves that all available Cr can be incorporated into the perovskite lattice. In sum, although the thermodynamic equilibrium was probably not yet reached for the sample $10LNF+1Cr_2O_3$ heated for 200 h at 800ºC in air, the reactivity between LNF and Cr_2O_3 was clearly demonstrated.
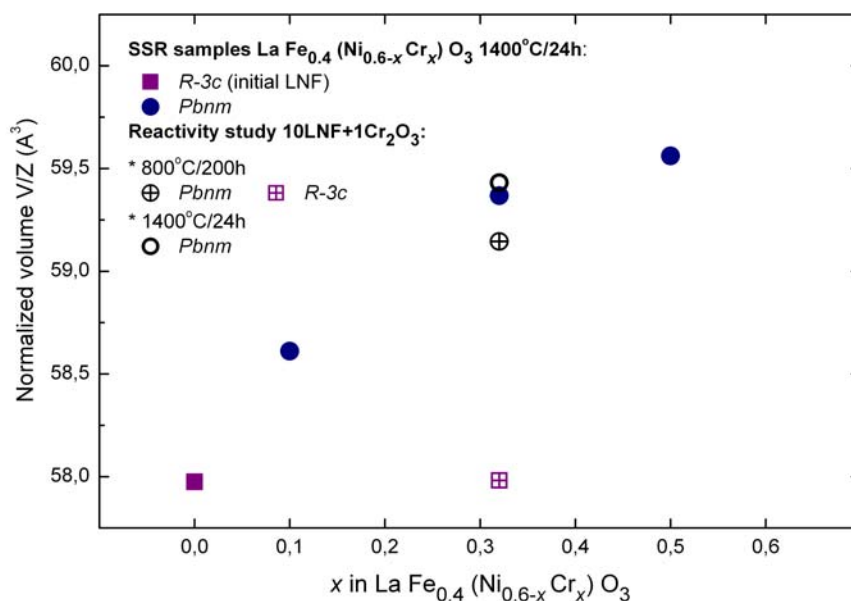

Figure 4. Variation of the normalized cell volume as the function of Cr amount in the $LaFe_{0.4}(Ni_{0.6-x}Cr_x)O_3$ series. Additionally, values for $10LNF+1Cr_2O_3$ samples are included.

Mixture $10LNF +3Cr_2O_3$ and $10LNF + 5Cr_2O_3$. XRD analysis of the heated (800ºC for 200 h) sample $10LNF+3Cr_2O_3$ showed the presence of NiO, a purely orthorhombic perovskite phase, and also a spinel phase (Fig. 5). The original rhombohedral LNF-phase was no longer observed, indicating a complete reaction of LNF with Cr_2O_3. In the heated $10LNF+5Cr_2O_3$ sample, the main phase detected was an orthorhombic perovskite phase, resembling the Cr-rich $La(Fe,Cr)O_3$ phase (Table I). This result suggests that first Ni is being replaced by Cr, followed by Fe-replacement. Next to this perovskite phase, a significant amount of a spinel phase was detected together with a trace amount of unreacted Cr_2O_3, while NiO was barely detected (Fig. 5). The spinel phase identified in the last two cases should generally be described as $(Ni,Fe)(Fe,Cr)_2O_4$. In the last two

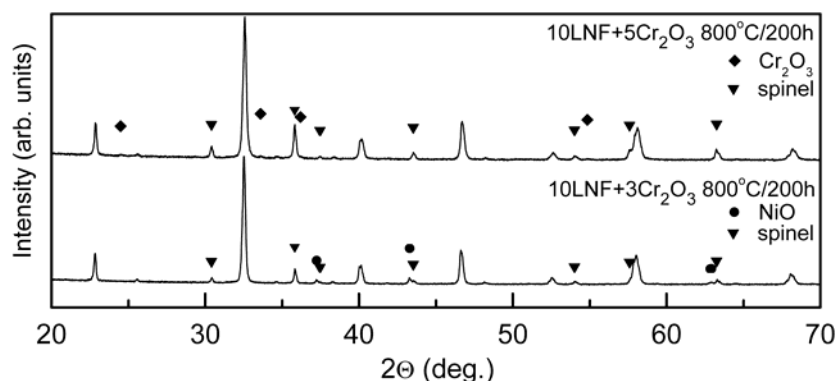samples, no rhombohedral LNF-phase was present either, again indicating a complete reaction of LNF with Cr_2O_3.

Figure 5. X-ray powder diffraction patterns of the mixtures $10LNF+3Cr_2O_3$ and $10LNF+5Cr_2O_3$ heated at 800ºC for 200 h.

The current study on reactivity between LNF and Cr_2O_3 at 800ºC demonstrates that chromium enters the perovskite phase, replacing first Ni and then Fe. The observed order of precipitation (first Ni, then Fe) from the initial LNF perovskite phase correlates well with the relative thermodynamic stability of the perovskites: $LaCrO_3 > LaFeO_3 > LaNiO_3$ (14). Substitution of Cr into the LNF lattice may result in a decrease of electronic conductivity, similar to what was reported for the $La(Ni_{1-x}Cr_x)O_3$ system (15). This might have serious implications for the ohmic losses across the LNF+Cr layer during fuel cell operation under the given conditions.

LNF and Cr_2O_3 Reactivity at 600ºC

The previous section showed that thermodynamic equilibrium in a mixture of LNF and Cr_2O_3 depends on temperature levels and exposure time. Equilibrium was not reached after 200 h at 800ºC, but increasing the temperature to 1400 ºC did result in equilibrium. Consequently, lowering the temperature is expected to hinder reactivity. Therefore, a similar reactivity study was conducted at 600ºC: first for 200 h and then for 1000 h. The XRD-analysis on the $10LNF+xCr_2O_3$ mixtures (x = 1, 3, 5) heated at 600ºC for 200 h and ultimately for 1000 h revealed no reaction between the two compounds: in all cases, only original LNF and unreacted Cr_2O_3 were found (Fig. 6). The application of LNF at 600ºC as a Cr-resistant cathode or contact coating would seem to be feasible, but this ought to be tested under long-term fuel cell operating conditions.

Conclusions

This study demonstrates the intrinsic instability of the LNF cathode when it is in direct contact with Cr_2O_3 at 800ºC. This situation may occur in the cathode compartment of a SOFC stack, when the Cr-containing metallic interconnect is in direct contact with this cathode or with contact coating material. The rate of the chromium reaction with LNF has been demonstrated to depend on temperature levels and exposure time. Lowering the operating temperature to 600ºC resulted in very low chromium reactivity with LNF: no reaction was observed with XRD. Thus, LNF at 600ºC would seem to offer promising opportunities concerning its use as a Cr-resistant cathode or contact coating. Nevertheless, further investigations remain necessary, especially under long-term fuel cell operation conditions.
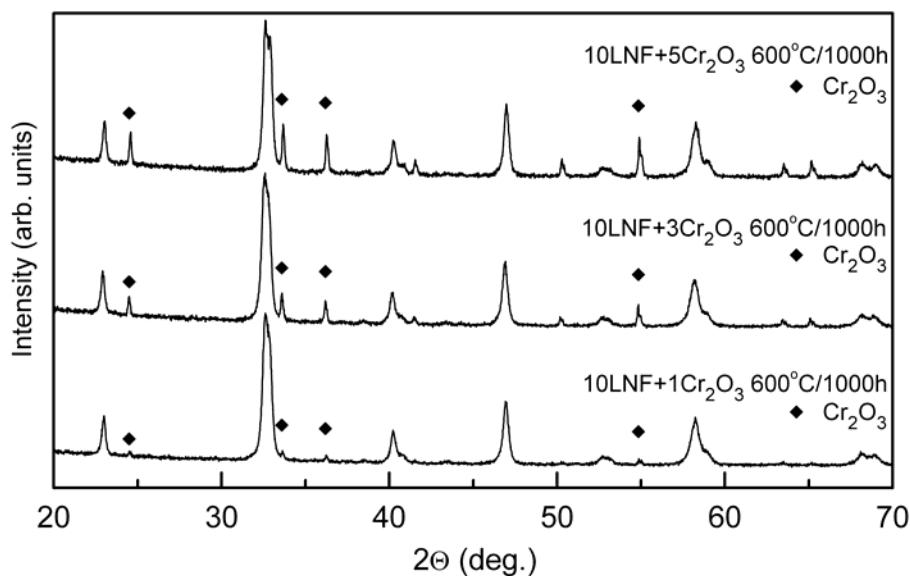
Figure 6. X-ray powder diffraction patterns of 10LNF+xCr$_2$O$_3$ mixtures (x = 1, 3, 5) heated at 600ºC for 1000 h.

Acknowledgments

References

1. J. Y. Kim, N. L. Canfield, L. A. Chick, K.D. Meinhardt, V. L. Sprenkle, *Ceramic Engineering and Science Proceedings*, **26**, No.4 (2005).
2. M. C. Tucker, H. Kurokawa, C. P. Jacobson, L. C. De Jonghe, S. J. Visco, *J. Power Sources*, **160**, 130 (2006).
3. T. Komatsu, H. Arai, R. Chiba, K. Nozawa, M. Arakawa, K. Sato, *Electrochem. Solid-State Lett.*, **9,** A9J (2006)
4. Y. D. Zhen, A. I. Y. Tok, S.P. Jiang, F.Y.C. Boey, *J. Power Sources*, **170,** 61 (2007).
5. R. Chiba, F. Yoshimura, Y. Sakurai, *Solid-State Ionics,* **124** (1999) 281-288.
6. F. P. F. van Berkel, M. Stodólny, M. Sillessen, J. P. Ouweltjes, *8th European Solid Oxide Fuel Cell Forum, Lucerne, Switzerland*, A0621 (2008).
7. M. Stodolny, F. P. F. van Berkel, J. P. Ouweltjes, *ECN internal Communication*.
8. A. Le Bail, H. Duroy, J. L. Fourquet, *Mat. Res. Bull.*, **23,** 447 (1988).
9. C. J. Howard, B .A. Hunter, A Computer Program for Rietveld Analysis of X-Ray and Neutron Powder Diffraction Patterns, Lucas Heights Research Labs, (1998).
10. H. Yokokawa, T. Horita, N. Sakai, K. Yamaji, M.E. Brito, Y.-P. Xiong, H. Kishimoto, *Solid State Ionics*, **177**, 3193 (2006).
11. T. Komatsu, H. Arai, R. Chiba, K. Nozawa, M. Arakawa, K. Sato, *J. Electrochem. Soc*, **154**, B379 (2007).
12. T. Hashimoto, N. Tsuzuki, A. Kishi, K. Takagi, K. Tsuda, M. Tanaka, K. Oikawa, T. Kamiyama, K. Yoshida, H. Tagawa, M. Dokiya, *Sol. State Ion.*, **132**, 181 (2000).
13. R. D. Shannon, *Acta Crystallogr. A*, **32**, 751 (1977).
14. J. Cheng, A. Navrotsky, X. Zhou, H. Anderson, *J. Mater. Res.*, **20**(1), 191 (2005).
15. H. E. Höfer, R. Schmidberger, *J. Electrochem. Soc.,* **141**, 782 (1994).